THE JOURNAL OF PHYSICAL CHEMISTRY B

Article

pubs.acs.org/JPCB

Probing Ultrafast Photochemistry of Retinal Proteins in the Near-IR: Bacteriorhodopsin and Anabaena Sensory Rhodopsin vs Retinal Protonated Schiff Base in Solution

Amir Wand,[†] Boris Loevsky,[†] Noga Friedman,[‡] Mordechai Sheves,[‡] and Sanford Ruhman*[,†]

[†]Institute of Chemistry and the Farkas Center for Light-Induced Processes, The Hebrew University of Jerusalem, Edmond J. Safra Campus, Givat Ram, Jerusalem 91904, Israel

[‡]Department of Organic Chemistry, The Weizmann Institute of Science, Rehovot 76100, Israel

Supporting Information

ABSTRACT: Photochemistry of bacteriorhodopsin (bR), anabaena sensory rhodopsin (ASR), and all-trans retinal protonated Schiff base (RPSB) in ethanol is followed with femtosecond pump−hyperspectral near-IR (NIR) probe spectroscopy. This is the first systematic probing of retinal protein photochemistry in this spectral range. Stimulated emission of the proteins is demonstrated to extend deep into the NIR, and to decay on the same characteristic time scales previously determined by visible probing. No signs of a transient NIR absorption band above $\lambda_{pr} > 1.3$ μm, which was recently reported and is verified here for the RPSB in solution, is observed in either protein. This discrepancy demonstrates that the protein surroundings change photochemical traits of the chromophore significantly, inducing changes either in the energies or couplings of photochemically relevant electronic excited states. In addition, low-frequency and heavily damped spectral modulations are observed in the NIR signals of all three systems up to 1.4 μm. By background subtraction and Fourier analysis they are shown to resemble wave packet signatures in the visible, stemming from multiple vibrational modes and by analogy are assigned to torsional wave packets in the excited state of the retinal chromophore. Differences in the vibrational frequencies between the three samples and the said discrepancy in transient spectra are discussed in terms of opsin effects on the RPSB electronic structure.

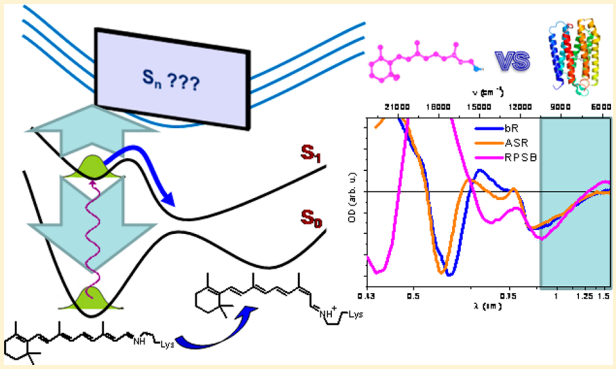

INTRODUCTION

Biological activity in all microbial retinal proteins (MRPs) is driven by photoabsorption in a common chromophore, the retinal protonated Schiff base (RPSB), which is covalently attached to a Lysine residue on the seventh helix.[1] In nearly all MRPs, absorption leads to photoisomerization of the retinal from all-trans to 13-cis on time scales ranging from a few hundred femtoseconds to several picoseconds. This triggers a protein-specific photocycle taking place on a millisecond time scale, and resulting in ion pumping or photostimulation. The most well-known MRPs are the bacteriorhodopsin (bR) and halorhodopsin (hR) ion pumps and the sensory rhodopsins SRI and SRII, all discovered in the archaeon *Halobacterium salinarum* several decades ago. Since then, genome sequencing has revealed an abundance of other MRPs in fungi, algae, and bacteria, making this one of the most abundant platforms for solar-energy bioutilization in nature.[2]

As the common motor for this expanding family of molecular machines, RPSB photochemistry has been the subject of extensive investigation, both in solution and more recently in gas phase isolation. The aim has been to characterize photochemical dynamics of RPSB outside the proteins and by comparison to reveal the role that the protein surroundings play on the course of photochemistry. This has shown the following: First, attachment to the protein tunes RPSB's absorption peak by thousands of wavenumbers compared to the solvated RPSB, giving rise to the so-called "opsin shift" which optimizes chromatic response to biological activity in each protein.[3,4] Second, the protein surroundings confine isomerization exclusively to the C_{13}═C_{14} double bond.[5] Third, it influences the isomerization efficiency, varying the quantum yields from a total of ∼20% in solution in all reactive channels to as much as ∼60% in the protein exclusive one: all-trans → 13-cis.[5−7] Despite their common architecture, significant variations are found within the MRP family, highlighting the specific role played by the protein surroundings on the chromophore photochemistry.

Photoisomerization in various MRPs and in RPSB has been studied by methods of ultrafast spectroscopy.[8−31] Time-

Special Issue: Paul F. Barbara Memorial Issue

Received: September 16, 2012
Revised: November 6, 2012
Published: November 9, 2012

resolving the rise and decay of excited state absorption and emission bands (to the "blue" and to the "red" of the ground state absorption, respectively) in MRPs not only demonstrates that internal conversion (IC) ranges from 0.5 to 10 ps but that, following an initial brief stage of spectral shifting,[25,30−33] this decay is kinetically describable as biexponential. This goes for the RPSB in solution as well, differing spectroscopically from the pigments in the blue shifting of the ground state absorption to the near UV. Aside from the significant variation in IC rates from one protein to another, an early suggestion that the briefness of IC is correlated with the subsequent efficiency of photoisomerization in the visible pigments does not appear to apply to their microbial relatives, as demonstrated in comparison of a few members of the family,[14,31,34,43,50,55] as well as in more recent works on related model systems.[35,36]

In order to rationalize these observations, a variety of models for the electronic surfaces involved have been proposed. These vary from two-state models (such as inertial, overdamped, or two-state two-mode models) to three-state models, which include at least one more electronic state in the photochemical stages.[10,30,37−42] The latter has been invoked to allow for the buildup, through avoided crossing, of a potential barrier along the reaction coordinate which could explain the slow biexponential excited state decay. It is also in line with spectral stagnation of the excited state during IC, further investigated by three pulse pump−dump−probe methods,[32,43] and with time-resolved fluorescence measurements of IC in RPSB solutions.[10,44]

The possible involvement of numerous excited surfaces in MRP photochemistry brings to mind the related family of carotenoids. Like the RPSB in retinal proteins, they are large conjugated polyenes, which among other functions act as photoreceptors in photosynthetic protein complexes. The involvement of multiple excited states in carotenoid photoreactivity is well-known and demonstrated clearly using femtosecond pump−near-IR (NIR) probe spectroscopy.[45] Significant differences in electronic structure and spectroscopy exist between the RPSB and carotenoids, due to the symmetry-breaking protonated Schiff base linkage.[46] This excludes drawing direct parallels between photochemical dynamics in both. Nonetheless, it is surprising that the NIR spectral region, which proved to be so helpful in understanding the photophysics of carotenoids, has been largely unexplored in the case of retinal proteins.

In an effort to remedy this oversight, Loevsky et al. have recently reported the first femtosecond pump−NIR probe (1−2 μm) study of RPSB in ethanol.[47] Following photoexcitation, it was shown that stimulated emission extends deep into the NIR, giving way to net absorption at wavelengths above 1300 nm. This absorption was demonstrated to decay in synch with the other excited state bands apparent in the visible. Despite the known overlap of excited state absorption and emission bands in the NIR, arguments were made in favor of assigning this new feature to a transition between the reactive excited state and a closely spaced additional excited singlet which is not involved in the other transitions observed to date.

It is important to test whether the same NIR absorption band appears in transient difference spectra obtained from MRPs as well. Here, we report the first extension of this femtosecond VIS−pump/hyperspectral NIR (0.9−1.6 μm)[48] probing approach to two MRPs, Bacteriorhodopsin and the anabaena sensory rhodopsin (ASR). The latter is the first sensory rhodopsin found in bacteria (cyanobacetrium *Anabaena (Nostoc) sp. PCC 7120*).[49] Its photoswitching reactive cycle is another unique trait,[6] recently shown to occur with very different rates in the primary steps in both switching directions.[50] In these two MRPs, following an ultrarapid (<50 fs) stage of spectral shifting and evolution, stimulated emission is observed to extend deep into the probed region. The long-wavelength (λ_{pr} > 1.3 μm) absorptive band, verified again to appear in excited RPSB, is absent in both proteins, pointing to opsin effects on RPSB electronic structure within both MRPs. The initial stage of evolution, which is mainly absorptive throughout the probed region, is discussed in light of theoretical predictions of the involvement of multiple excited states on the way to the conical intersection. The improved S/N ratio also allowed for extraction of excited state vibrational coherences signatures deep into the NIR and for direct comparison of these between the three systems, pointing at the decisive role of the surroundings on these collective torsional motions of the backbone of the retinal.

EXPERIMENTAL SECTION

Sample Preparation and Handling. All samples were prepared following known procedures, as briefly described next:

RPSB. All-trans RPSB in ethanol solution was prepared as previously described.[17] Briefly, aldehyde was mixed with an excess of *n*-butylamine (10 equiv) in ethanol for 1 h. The ethanol and excess of amine were evaporated, and the residue was dissolved in ethanol and acidified with a dilute solution of trichloro acetic acid. Complete protonation and subsequent stability of the reactant were monitored by absorption spectroscopy. In order to minimize oxidation of the sample during storage it was kept under nitrogen, in the dark, at a temperature of −30 °C.

bR. Halobacterium salinarum was grown from the S9 strain, and purple membranes containing bacteriorhodopsin were isolated as previously described.[51] Potassium phosphate buffer was used to maintain a neutral pH.

ASR. ASR samples were prepared according to previously published methods,[49,52] with the full details found in ref 50. Briefly, ASR was expressed in *Echerichia coli* strain UT5600. Grown cells were induced with 1 mM IPTG and 10 μM all-trans-retinal overnight. Pink-colored cells were harvested by centrifugation, resuspended in 50 mM buffer Tris-HCl, and recentrifuged at 18,000 rpm. Precipitated cells were suspended with buffer S containing 1% *n*-dodecyl-β-D-maltoside (DDM), and lysed with lysozime (0.1 mg/mL) in the presence of DNase at room temperature overnight. Extracted protein, collected as supernatant, was purified by using a Ni^{2+}-NTA agarose column and then washed with buffer W and eluted with buffer E. Eluted protein was washed and concentrated with buffer phosphate (50 mM, pH 7.5) containing 0.06% DDM, using Amicon ultra centrifugal filter devices.

Room temperature samples with a nominal OD of 0.4−0.7 at the excitation wavelength (see normalized absorption spectra in Figure 1) were syringe pumped through a ∼0.4 mm path length cell, equipped with 0.2 mm fused silica windows. RPSB and ASR experiments were conducted with red-filtered lab illumination to eliminate unwanted photoisomerization. bR samples were irradiated with white light from a 150-W quartz halogen fiber bundle light source for ∼15 min prior to the experiment, and continuously light adapted during pump−probe measurements, maintaining a >95% all-trans retinal composition. ASR samples were kept in the dark overnight

dx.doi.org/10.1021/jp309189y | J. Phys. Chem. B 2013, 117, 4670−4679

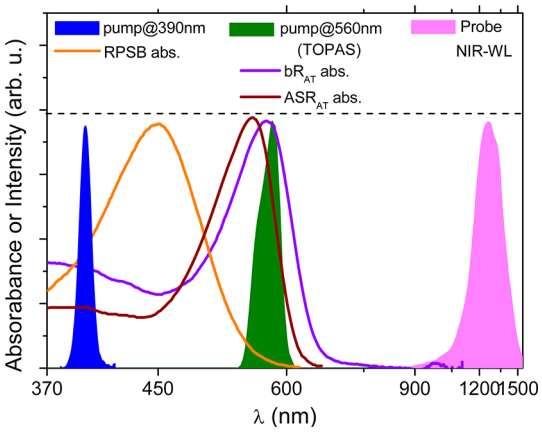

Figure 1. Absorption spectra of all-trans bR, ASR, and RPSB. Intensity spectra of pump and probe pulses employed in experiments are portrayed as well (see text for details).

prior to measurements to obtain an all-trans sample with similar isomeric purity.

Pump−Probe Measurements. Pump−probe runs were conducted using methods of pulse generation and intensity controls described in refs 47 and 50. Pulses of ∼30 fs duration and centered at 790 nm which were derived from an amplified titanium sapphire laser were used to generate pump and probe pulses. Pump pulses were ∼25−35 fs in duration centered either at 390 nm (for RPSB) by doubling the amplifier output in a 200 μm BBO crystal, or at 560 nm (for bR and ASR) as produced in an optical parametric amplifier (TOPAS, light conversion). Supercontinuum probe pulses were generated by focusing ∼1 μJ of the 790 nm fundamental in 2.5 mm of sapphire. Typical excitation and probing spectra are depicted in Figure 1. Both pulses were focused with reflective optics into the samples, with the probe going through a VIS cutoff filter (FEL0900, Thorlabs). Typically, a 40−70 nJ pump beam focused to a spot size of 200 μm in diameter was overlapped

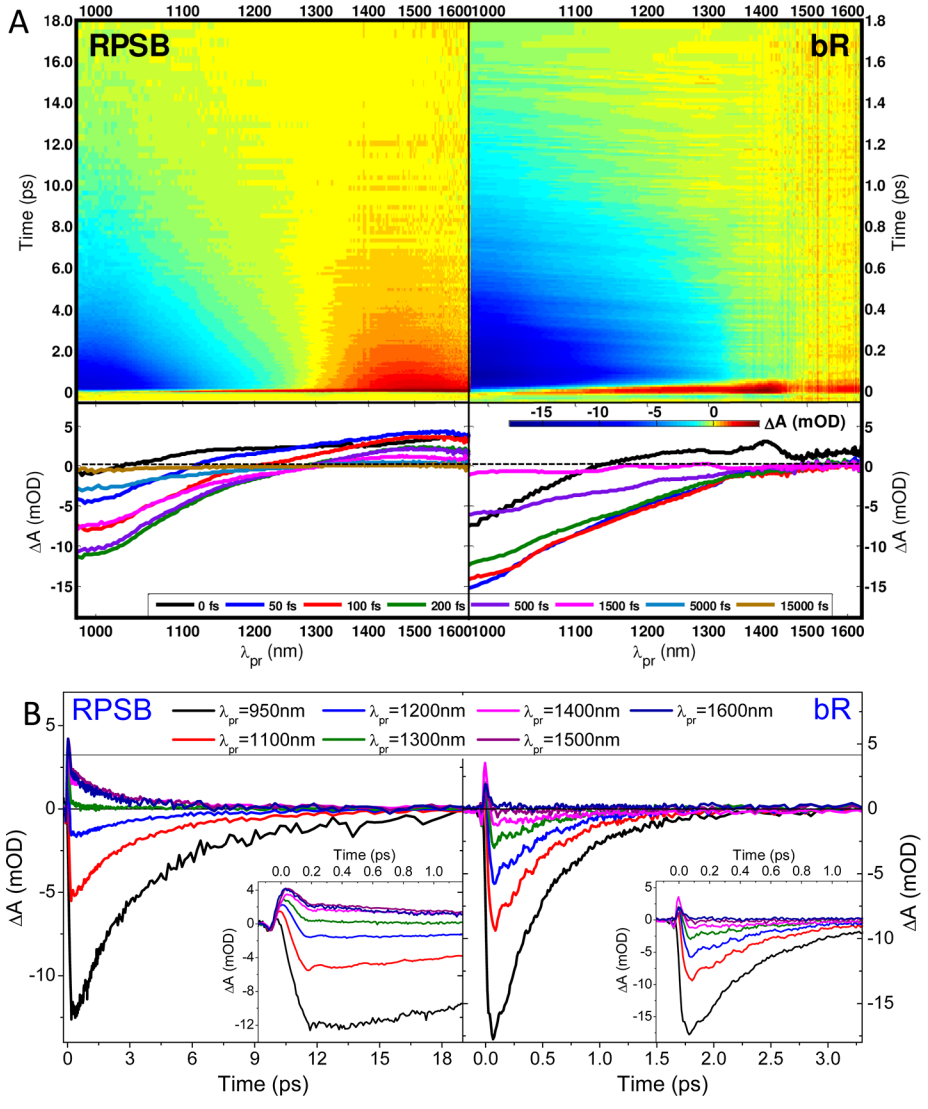

Figure 2. (A) Transient difference absorption spectra of RPSB (left panels) and bR (right panels), corrected for group delay dispersion of the probe, and presented as color-coded maps of the ΔOD as a function of probing wavelength and pump−probe delay. Lower panels depict a series of transient spectra (horizontal cuts in the map above) at the designated pump−probe delays. (B) A series of ΔOD kinetics at selected probing wavelengths (vertical cuts in the maps). Insets present initial 1 ps of pump−probe delay. Note different time scales for RPSB and bR in panel A maps and in panel B main frames.

dx.doi.org/10.1021/jp309189y | J. Phys. Chem. B 2013, 117, 4670−4679

with a probe beam ~2 times smaller in size; these were verified to give signal amplitudes linear in pump intensity up to 2−3 times than that used in reported results. After passing through the sample, the transmitted probe was fed into an InGaAs array spectrograph covering a spectral range between 0.9 and 1.7 μm (BTC261E, B&W TEK, USA). Consecutive pump-on/pump-off pulses were averaged and used to calculate the wavelength-dependent optical density difference spectra ($\Delta OD(\lambda,t)$). Dispersion of pump pulses was compensated for in a slightly misaligned zero-dispersion grating pulse shaper. Obtained spectra were time-corrected for group dispersion of the probe continuum based on Kerr scans,[53] leading in total to an average effective time resolution of ~70 fs throughout the probing spectral region.[54]

RESULTS AND ANALYSIS

A. Ultrafast Pump−Probe Data for RPSB, bR, and ASR. Figure 2A depicts time-corrected transient absorption spectra as a function of time and wavelength ($\Delta OD(\lambda,t)$) for RPSB (left) and bR (right) as color-coded contour maps. The lower panels present a set of transient spectra, which are cuts at the designated pump−probe delay times in the maps above. Current results for RPSB closely reproduce those reported in our earlier study.[47] Briefly, immediately following photoexcitation an ultrabroad short-lived absorption is apparent throughout most of the probed range. While this signal shifts within 100−200 fs to stimulated emission for λ_{pr} < 1.3 μm, continued absorption is seen at longer wavelengths. At even longer delays the signal decays across the board, preserving an isosbestic point near 1.3 μm. These observations are further clarified in the temporal and spectral cuts below the map and in panel B of the same Figure.

As in the case of RPSB, bR transient spectra start with a short-lived (<100 fs) absorption for λ_{pr} > 1.1 μm. Unlike RPSB, this reverts to stimulated emission throughout the probed region, reducing in intensity toward the red, without the appearance of an absorption growing in above 1.3 μm. The decay of the observed emission proves that it is the extension in the NIR of the known S_1 excited state emission of bR (see Figure 3). This finding demonstrates yet again that attachment to the opsin alters the photophysics and chemistry significantly, in this case either shifting or modifying the transition dipole strengths of various excited state absorption bands observed for RPSB in solution.

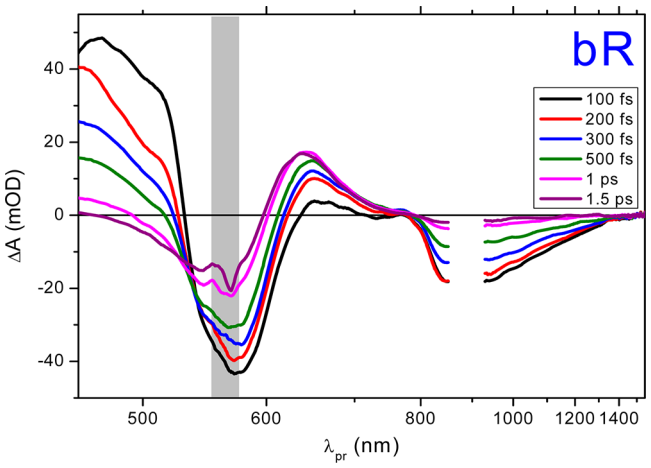

Figure 3. Transient ΔOD spectra at designated delays after excitation of bR, probed from 450 to 1500 nm (VIS data are based on ref 31). Shaded area designates range obscured by scattered pump radiation.

Similar findings, including the early absorption shifting to a decaying emission band, were observed for the ASR as well, and are summarized briefly in Figure 4 and further portrayed in the Supporting Information (text and Figures S1−S2). The main difference between the two proteins pertains to the slower and more markedly multiexponential character of IC in ASR,[50] observed in other MRPs (e.g, Halorhodopsin) as well.[43,55]

Finally, a close look at single wavelength absorption changes reveals low-frequency heavily damped modulations in the signal (with periods of ~200−300 fs) on top of the kinetic traces in all three samples (see Figures 2B and 4C), which are discussed below in detail.

B. Global Fitting of bR and ASR Data. Global fitting was conducted both to conveniently parametrize the data and to demonstrate the similarity of the resulting decay times with those characteristic of IC kinetics measured in the visible. RPSB experiments were in line with our earlier study described in ref 47. Once convoluted with an experimentally determined instrument response function, and superimposed with an instantaneous artifact response, data from the two proteins were adequately described with a sequential kinetic scheme as follows:

$$A^* \xrightarrow{1/\tau_1} A_1^* \xrightarrow{1/\tau_2} A_2^* \xrightarrow{1/\tau_3} B$$

The obtained evolution associated difference spectra (EADS) and matching decay times are shown in Figure 5 and Figure S3 in the Supporting Information (bR) and in panel B of Figure 4 (ASR). This scheme was chosen since it is the simplest one necessary for high quality fitting of the data and following the previously mapped multiexponential kinetics of MRPs. Furthermore, the same quality of fitting could be obtained with a parallel kinetic scheme, and our choice of sequential kinetics was chosen primarily for simplicity of interpretation.

For the case of bR, two components (along with the coherent-coupling component) were found sufficient to describe the data well (eliminating the need for the step forming A_2^*). The decay times observed, in particular the dominant ~0.5 ps component, are in agreement with those obtained from visible probing measurements, demonstrating compatibility with the interpretation of the signal which supersedes the initial spectral shifts as a continuation of the S_1 stimulated emission band. The preceding sub-100 fs component is also in line with observations in numerous ultrafast spectroscopic studies on MRPs in the VIS,[19,26,31,43,44,50,55] and with recent observations of an even shorter component in the RPSB when probed in the NIR.[47] Whether this feature results from absorption between closely spaced excited states as previously suggested for RPSB, or is due to a coherent wave mixing, was addressed here within the context of the global fitting and by comparing the data to pure solvent pump−probe runs. Separation between these possibilities is hampered by current limited temporal resolution, and should be addressed in future studies using <10 fs pulses. The results of the current analysis, presented in the Supporting Information, do however favor the existence of a short-lived excited state intermediate, in line with the recent study of the RPSB.[47] It is important to point out that even if this early absorption is partially due to nonlinear wave mixing, its sign and prominence away from ground state resonance demonstrates the existence of absorptive resonances of the bR in the

dx.doi.org/10.1021/jp309189y | J. Phys. Chem. B 2013, 117, 4670−4679

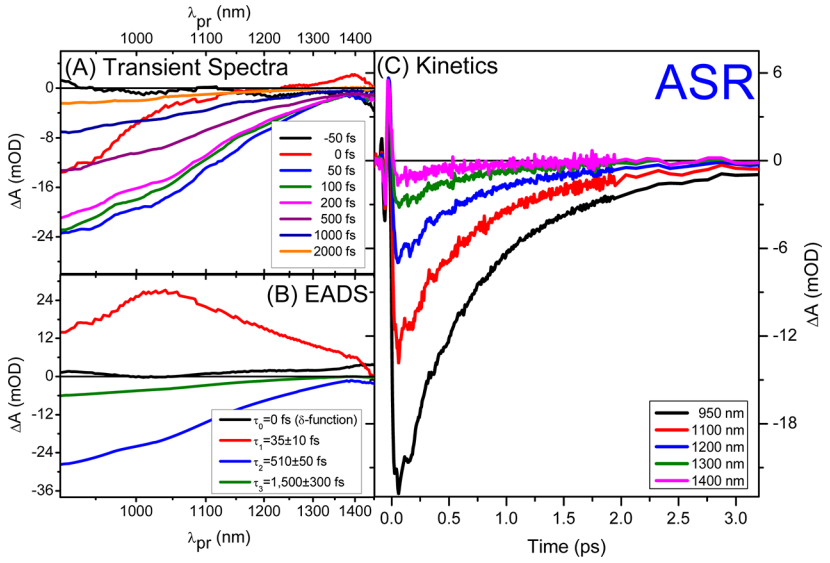

Figure 4. Results of VIS-pump–NIR-probe experiments on dark-adapted anabaena sensory rhodopsin (>97% all-trans). Panels A and C present series of transient spectra and single wavelength kinetics at designated probe delays and wavelengths, respectively. Panel B presents global kinetic fitting analysis of this data in terms of EADS using the model described in text (see also pages S2–S5 in the Supporting Information).

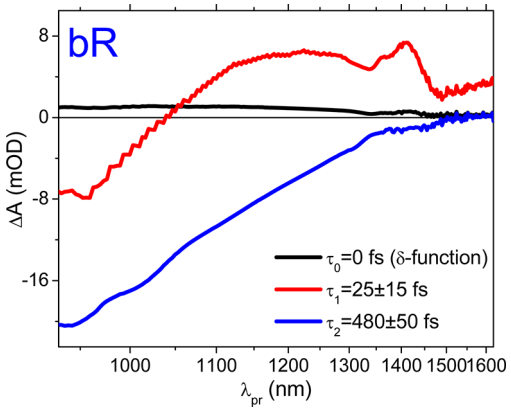

Figure 5. bR evolutionary associated decay spectra (EADS) and their time constants, derived by global fitting to the sequential kinetic scheme found in the text. The τ_0 component (shown in black line) represents instantaneous coherent coupling of pump and probe pulses. See also pages S4–S5 in the Supporting Information.

NIR, as can be deduced from a perturbative description of pump–probe spectroscopy, lending further support to this analysis.[56]

Panel B of Figure 4 presents the global fit analysis using the same model for the data of ASR. Compared to the bR, the ASR data demand the inclusion of a third component, leading to a biexponential decay as observed in, e.g., hR and SRs.[14,43,55] In addition, here too an absorptive <50 fs component dominates early delay times.

Current results highlight a specific strength of probing MRP photochemistry in the NIR spectral region. This range is free of spectral overlap with ground-state reactant and product spectra, allowing selective probing of the excited state. It also suggests that numerous decay stages frequently used to fit VIS-probing results of bR most likely reflect simultaneous ground state cooling and photoproduct evolution, and not complex and multistaged IC of the excited-state.

C. Excited State Vibrational Coherences of the Retinal Backbone. The data sets of the solvated RPSB and of both MRPs include weak damped periodic modulation patterns in the initial ~1 ps following photoexcitation. These were extracted and characterized in the time and frequency domains.[57] First, they were isolated from the pump–probe data by subtracting a multiexponential kinetic fit from the raw data to obtain the residuals: $\Delta R(\lambda,t)$, which are shown for RPSB and bR as color-coded contour maps in panel A of Figure 6 in the left and right panels, respectively. The residuals were then Fourier transformed in the pump–probe time window 100 fs < t < 1500 fs to obtain power spectra presented as a function of probe wavelengths in the form of a two-dimensional map in panel B of the same figure. Panel B also contains the wavelength-integrated (λ_{pr} = 950–1450 nm) power spectra of all three samples, highlighting the vibrational modes observed in each.

Structure in the Fourier power spectra of RPSB's modulations suggests a prominent oscillation at ~120 cm^{-1} and a weaker 250 cm^{-1} contribution, and at least two components at 160 and 210 cm^{-1} for bR. In the case of ASR, along with peaks similar to those observed for bR, a strong additional feature in the Fourier mapping of modulations at the selected wavelength is observed at 300 cm^{-1} as well. Caution must be taken when interpreting IVS signals from rapidly damped vibrations since overlapping interferences as well as probe wavelength-dependent harmonics can mask simpler vibrational structure. In order to further characterize the observed modulations and their dynamics, a sliding-window Fourier transform (SWFT) analysis has been performed on the same residuals. Since undulations in all probing wavelengths have a similar absolute phase,[58] an averaging of residuals over λ_{pr} = 1000–1400 nm was performed prior to the Fourier transformations. Typical resulting spectrograms are depicted in Figure 7 for RPSB and bR in the left and right panels, respectively, using a super-Gaussian (SG) window of 400 fs (fwhm) width. These plot the Fourier amplitude as a function of the window position with respect to the pump–probe delay.

The spectrograms are compatible with multimode contributions to the modulations from modes with typical dephasing

dx.doi.org/10.1021/jp309189y | J. Phys. Chem. B 2013, 117, 4670–4679

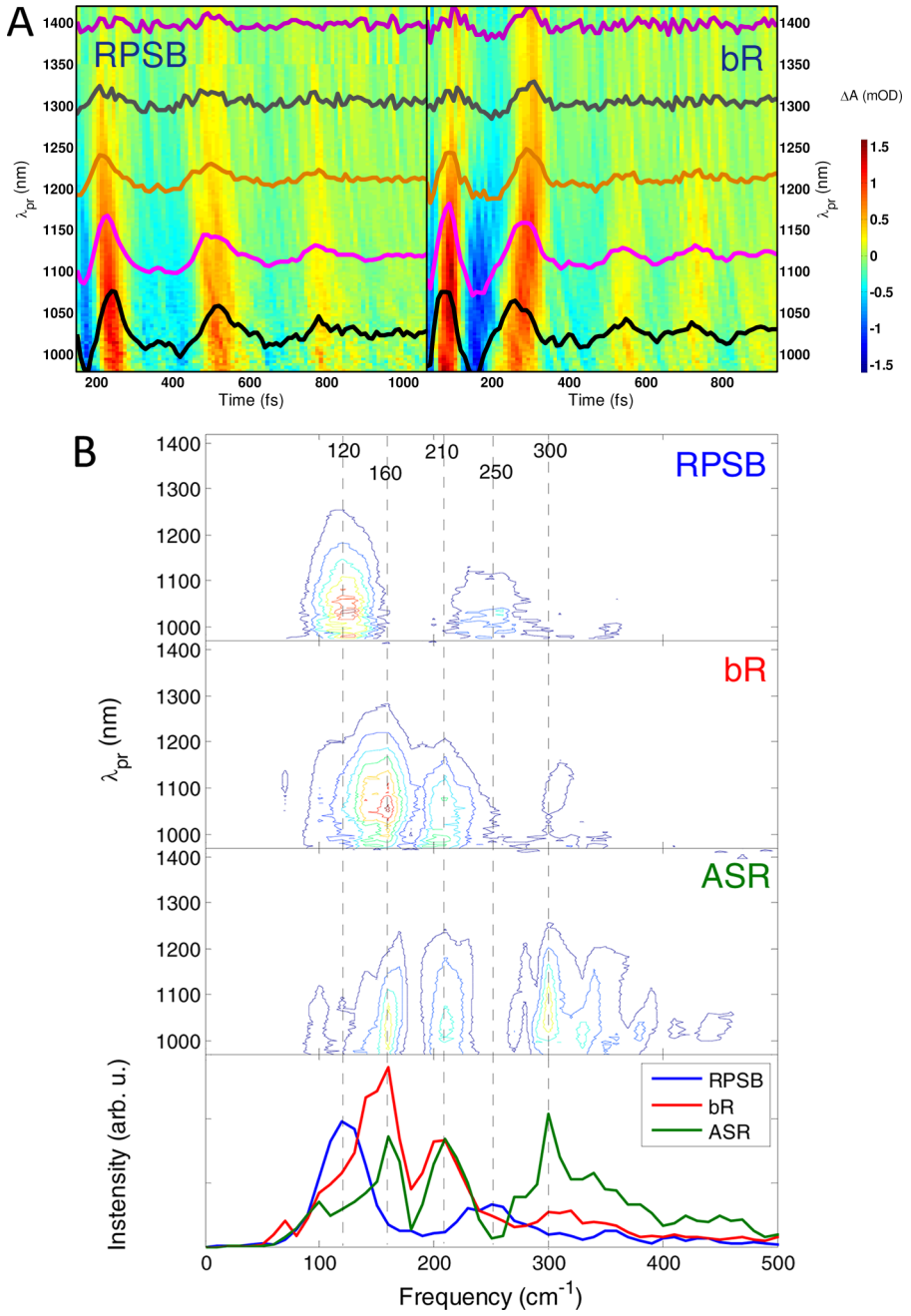

Figure 6. Time domain (A) and frequency domain (B) representations of excited state vibrational coherences. (A) The residuals ($\Delta R(\lambda,t)$) of RPSB and bR, obtained by subtraction of the kinetic fits from the raw data, are presented as color-coded contour maps. Residuals at selected probe wavelengths (λ_{pr} = 1000, 1100, ..., 1400 nm) are overlaid on the contour maps. (B) The frequency domain mapping of (A), obtained by discrete Fourier transformation (DFT). The three upper panels present contour maps for RPSB, bR, and ASR, respectively, while the lower depicts the integrated intensity of the DFT maps over λ_{pr} = 950−1450 nm.

times of a few hundreds of femtoseconds. Special care, however, should be put into the interpretation of SWFT data, especially with relatively narrow windows and/or closely spaced multimode contributions.[59,60b] In both RPSB and bR, the higher frequency modes (around ∼250−300 cm^{-1}) dephase on faster time scales. Although some allegedly dynamic downshifting of the frequencies with time is apparent, it is tentatively assigned to contributions from two different closely lying modes, as demonstrated in the Supporting Information and discussed below.

DISCUSSION

The two central findings of this study are (a) that, unlike the isolated RPSB, bR and ASR lack an excited state absorption band extending deeper in the NIR, beyond the stimulated emission from S_1 to S_0, and (b) the observation and characterization of coherent wave packet modulations deep in the near-IR.

Observation (a) is summarized in Figure 8, which presents the full VIS-NIR transient absorption spectra for bR, ASR, and RPSB at ∼200 fs time delay after photoexcitation using the relevant excitation pump (see Figure 1 and the Experimental

dx.doi.org/10.1021/jp309189y | J. Phys. Chem. B 2013, 117, 4670−4679

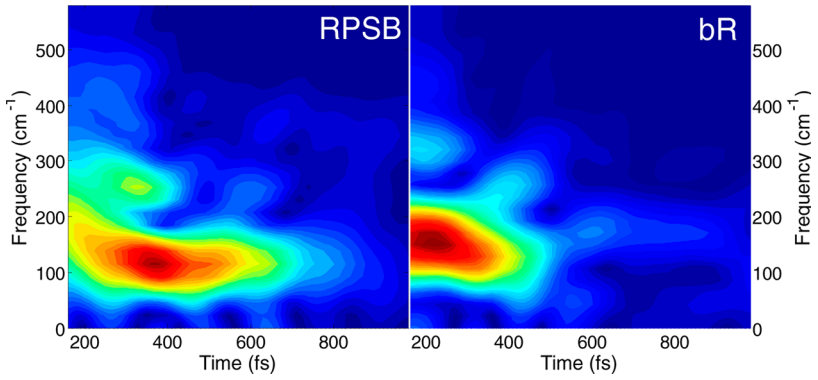

Figure 7. Sliding window Fourier analysis of spectral modulations, as derived from spectral averaging of the isolated residuals (Figure 6A) along λ_{pr} = 1000−1400 nm, for RPSB (left) and bR (right). Spectrograms were obtained using super-Gaussian windows with fwhm temporal width of 400 fs.

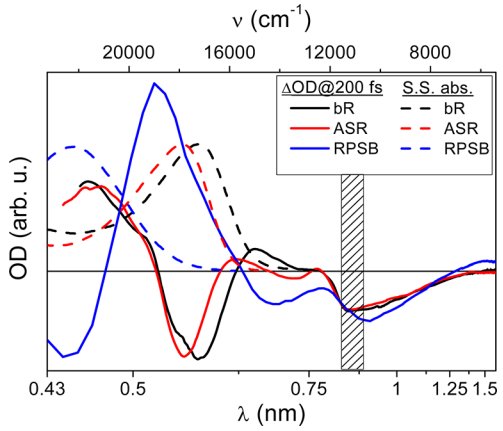

Figure 8. Transient spectra at pump−probe delay of 200 fs for RPSB, bR, and ASR (solid lines), following excitation with a relevant pump (see Figure 1). VIS-probing range adapted from refs 17, 31, and 50. Steady state absorption spectra of the three samples are depicted in dashed lines. The transient absorption curves were normalized to similar ground state bleach depth for convenience.

Section). The spectra were obtained by combining current data with previous VIS-probing studies (refs 17, 31, and 50 for RPSB, bR, and ASR, respectively). As discussed in ref 47, the existence of an absorptive band in the RPSB which decays in synch with the visible absorption and red emission bands assigned to S_1 demonstrates its connection with the photochemically active excited state. The identity of the potential surface to which this NIR absorption takes place in excited RPSB remains unknown. The possibility of this absorption band involving the same electronic state as that giving rise to the transient bands near 780 nm, which are partially overlapping with stimulated emission in the proteins and in RPSB, was deemed remote. Therefore, these results prove only the existence of an allowed optical transition to a singlet state near S_1, possibly broadened by the narrowing of interstate spacing in the vicinity of a conical intersection.[61] A recent theoretical study suggested the assignment of these to a $S_1 \rightarrow S_2$ transition near the conical intersection, which was predicted for solvated RPSB, and for bR as well.[62] Interestingly, the study also predicts that for bR the energy gap might be considerably lowered, thus shifting its absorption to deeper in the NIR. Probing in that region is, however, not experimentally feasible in aqueous environments,[48] and also renders such an hypothetical transition photochemically irrelevant in the proteins.

The sub-100-fs spectral evolution stage, which was detected in all samples, has been reported following high time resolution ultrafast photoexcitetion experiments in the VIS for MRPs,[25,30−33,50] and in the solvated RPSB.[10,17,19,20,44] The considerable spectral evolution observed during this stage was interpreted as reflecting initial structural changes or relaxation of the retinal.[63−68] In the case of RPSB, a recent time-resolved fluorescence study suggested that excitation at 400 nm leads to involvement of at least two singlet excited states, S_1 and S_2, in which a sub-100-fs (~50 fs) initial relaxation takes place.[10] This is compatible with a possibility considered in our previous report on the NIR probing of RPSB photochemistry, that in analogy with the primary steps in the photochemistry of carotenoids, this is an initial ultrafast stage of IC.[45,47] The theoretical work presented above suggests an additional point of view, in which, while the two-state, two-mode picture generally applies for both bR and solvated RPSB, an Ag-like (S_2) state might mix with the Bu-like (S_1) state just after photoexcitation, giving rise to a transient absorptive signal.[62] Thus the assignment of this phase of evolution requires further scrutiny.

The other noteworthy observation is the detection of low-frequency and heavily damped vibrational coherences in all three systems. Theses spectral modulations, observed here in NIR transient absorption, are assigned to torsional motions in the electronic excited state,[69,70] as previously described using VIS pump−probe data for a variety of MRPs (bR, ASR, hR, and pR) and for the RPSB.[43,50,69,71−74] This analysis was bolstered by appearance of similar modulations in time-resolved fluorescence experiments,[10,44] and in four-wave-mixing (FWM) experiments.[60] Verification based on the dependence of their phase and amplitude on probing wavelength, and comparison to resonance Raman (RR) experiments,[75] further supported this assignment. Although some experiments have concluded that the observed modes do not directly relate to the "reactive" torsional motion around the C_{13}=C_{14},[59,76] recent coherent control studies on bR maintain that they play a decisive role in gaining access to the reactive curve crossing to the ground electronic surface.[77] Therefore, they serve as important indicators of the primary structural evolution of the retinal chromophore, either solvated or inside the protein surroundings, and may aid in extracting information about the topology of photochemically active excited electronic states.[76] Whether they are directly excited by the optical transition or due to coupling to the reaction coordinate outside the Franck−Condon (FC) window remains debatable.[39,44b,60a]

dx.doi.org/10.1021/jp309189y | J. Phys. Chem. B 2013, 117, 4670−4679

Current measurements extend the previous VIS reports of these oscillations much deeper in the NIR. As discussed extensively elsewhere, such wave packet signatures in pump−probe data can reflect periodical changes in real or imaginary parts of the index and for the latter appear in signatures of excited state absorption or emission known to coexist in this spectral region.[56,78] These discussions show that for low frequency modes, the spectral signatures of either contribution, i.e. absorptive or dispersive, will fall off rapidly with detuning from the transition. Thus the observation of strong modulations at wavelengths so far from the ground state absorption band conclusively confirms their assignment to an excited state. This is further supported by the wavelength-dependent amplitude profile of the modes, supporting their assignment to an optical transition peaked at ∼900 nm. In the case of bR and ASR, this must be stimulated emission. We note in passing that the similarity in wavelength dependence of modulations observed in the pigments and RPSB solutions is at odds with them stemming from the absorption band which is observed only in the latter. The reason for absence of observable modulations in that band is not clear but might reflect different mode displacements in the responsible S_1-S_n transition.

As in all impulsive vibrational signals, phase is helpful in determining their origin. As shown in Figure 6A, the initial phase is essentially unchanged from 1π across the probed range,[58] which proves that the vibrations originate from the excited state and from the same electronic transition band, most likely that of stimulated emission, probed on the "red" with respect to its peak. The slight changes in the peak positions of the leading modulations, observed mainly in the probing between 950 and 1100 nm (Figure 6A), most likely reflect wavelength-dependent admixtures of different oscillating contributions, and are not mainly due to experimental error in determination of time zero, which was verified to be within ±20 fs.

The detailed structure of the vibrational power spectra is worthy of additional comment. Some earlier experiments have interpreted modulations in visible transmission data in terms of one central frequency, being ∼120 cm^{-1} for the RPSB and ∼170 cm^{-1} for the bR. In others, the involvement of multiple low-frequency modes has also been suggested.[60,69,70,72] Our current results are in good agreement with the modes extracted recently using VIS-FWM on bR and RPSB by Kraack et al.[60] For the bR, however, as off-resonance contributions of the ground state are expected to be vanishingly low in the current probing range (∼5000 cm^{-1} away from the ground state absorption), our results suggest that the modes around ∼300 cm^{-1} could also be assigned to excited state wavepacket motion, in spite of their proximity to the ground state mode (measured by resonance Raman)[75] and contrary to the interpretation given there.[60b] According to our results, this mode dephases faster than others. Regarding the RPSB, the wavelength-dependence of amplitude, and the relative rates of dephasing,[79] suggest that the 250 cm^{-1} is the reflection of the second harmonic of the leading 120 cm^{-1} vibration, as previously suggested,[71] rather than of a different normal mode of the retinal.

The differences in modulation frequencies demonstrated in Figures 6 and 7 deserve mentioning. These modulations are almost solvent-independent for the case of RPSB[10,76] but are significantly varied between different MRPs. They were suggested to reflect protein-specific interactions with the retinal, probably due both to steric effects and electrostatic forces, influencing its initial configuration and torsional potential and altering the photochemical dynamics. The similarity of modulations observed in bR and ASR does not carry over to all MRPs. In the case of hR, for instance, similar modulations are lowered below 100 cm^{-1} for the pigment relative to the free RPSB, demonstrating that this aspect is protein-specific.[43] In line with the earlier comparative study, this may reflect increased rigidity of the retinal conformation in bR and ASR and softening of it in the case of hR.

SUMMARY AND CONCLUDING REMARKS

Ultrafast (<100 fs resolution) hyperspectral transient absorption spectra in the NIR were recorded and compared for the retinal chromophore, either solvated in ethanol (RPSB) or within two microbial rhodopsins: bacteriorhodopsin and anabaena sensory rhodopsin. This spectral region, not previously investigated, shows significant differences between transient spectra observed in the retinal and those obtained from the proteins, while also allowing isolation and detailed characterization of their excited state signals.

The transient absorption band appearing deep in the NIR (λ_{pr} > 1.3 μm), reported recently for RPSB and corroborated here, is absent from transient absorption experiments with the two proteins. This demonstrates again that the opsin induces significant changes in the electronic structure of the retinal chromophore, altering the ordering, energies of transition dipole strengths. Further experimental and theoretical work is needed to reveal the origin and nature of the induced changes. Higher temporal resolution experiments are needed to aid in resolving the initial ∼100 fs following photoexcitation, in which spectral evolution was tentatively observed in all systems.

Moreover, the signatures of slow torsions of the backbone of the retinal, not reported before in this spectral region, were compared for all systems, reflecting the wavepacket dynamics on the excited states. Differences between the systems, as well as multimode contributions from torsional modes, point at alterations of the early dynamics. Finally, we note that the NIR probing region, being dominated by excited state signals, may prove promising for future studies of the higher-frequency modes, especially those connected with C−C and C═C bond stretching of these photoisomerizing systems. This has been difficult in the visible due to extensive overlap with ground state absorption and, if successfully applied in the NIR, might unravel the role played by specific structural changes and functional groups in the multidimensional dynamics and reaction coordinates of these proteins.

To summarize, all of these observations contribute significantly to the ongoing quest for appreciating protein effects on RPSB photochemistry. Starting with the obvious tuning of the S_0-S_1 absorption band, current results complete a VIS-NIR mapping of nascent excited state difference spectra in the free chromophore and in a series of natural microbial pigments. They demonstrate that theoretical simulations of the electrostatic modulation of energy gaps underlying MRP opsin shifts, which predict shifts in other excited state signatures, are not observed experimentally and require revision and modification. Demonstrating this has required the full mapping of excited state absorption and emission as demonstrated in earlier publications from our lab and others. The end result, prior to this installment, was that nearly all bands, other than the ground state absorption, remain basically fixed in frequency space upon electronic excitation in the visible, and that

dx.doi.org/10.1021/jp309189y | J. Phys. Chem. B 2013, 117, 4670−4679

presence of the protein surroundings significantly impacts low frequency vibrational wave packet motions unleashed in the excited state. The reported observations identify an additional significant difference in electronic excited state bands between RPSB solutions and the pigments deep in the NIR, where absorption rises exclusively in the former but not in the proteins studied. Along with the excited state torsional dynamics characterized more precisely by observations in the NIR, these findings provide new constraints for advanced quantum chemical simulations of RP photochemistry which should prove invaluable in directing theory in the right direction.

■ ASSOCIATED CONTENT

Supporting Information

Summary of ultrafast pump−probe results for anabaena sensory rhodopsin, more information regarding the global fitting procedure of bR ad ASR, detailed analysis of the initial ∼100 fs signals in all systems, and discussion on the SWFT analysis. This material is available free of charge via the Internet at http://pubs.acs.org.

■ AUTHOR INFORMATION

Corresponding Author

*E-mail: sandy@mail.huji.ac.il. Tel: +972-2-6585326. Fax: +972-2-5618033.

Notes

The authors declare no competing financial interest.

■ ACKNOWLEDGMENTS

This work was supported by the Israel Science Foundation (ISF), which is administered by the Israel Academy of Sciences and Humanities, and the U.S.−Israel Binational Science Foundation (BSF). A.W. is supported by the Adams Fellowship Program of the Israel Academy of Sciences and Humanities. M.S. holds the Katzir-Makineni chair in chemistry and is supported by the Kimmelman center for Biomolecular Structure and Assembly. The Minerva Farkas Center for Light-Induced Processes is supported by the Minerva-Gesellschaft für die Forschung GmbH, München, Germany.

■ REFERENCES

(1) (a) Spudich, J. L.; Yang, C. S.; Jung, K.-H.; Spudich, E. N. *Annu. Rev. Cell Dev. Biol.* **2000**, *16*, 365−392. (b) Spudich, J. L. *Trends. Microbiol.* **2006**, *14*, 480−487.

(2) (a) Venter, J. C.; et al. *Science* **2004**, *304*, 66−74. (b) Zhang, F.; et al. *Cell* **2011**, *147*, 1446−1457.

(3) (a) Nakanishi, K.; Balogh-Nair, V.; Amaboldi, M.; Tsujimoto, K.; Honig, B. *J. Am. Chem. Soc.* **1980**, *102*, 7945−7947. (b) Erbey, T.; Koutalos, Y. *Prog. Retin. Eye Res.* **2001**, *20*, 49−94. (c) Kloppmann, E.; Becker, T.; Ullmann, G. *Proteins: Struct., Funct., Bioinf.* **2005**, *61*, 953−965. (d) Hoffmann, M.; Wanko, M.; Strodel, P.; Konig, P. H.; Frauenheim, T.; Schulten, K.; Thiel, W.; Tajkhorshid, E.; Elstner, M. *J. Am. Chem. Soc.* **2006**, *128*, 10808−10818.

(4) Rajput, J.; Rahbek, D.; Andersen, L.; Hirshfeld, A.; Sheves, M.; Altoè, P.; Orlandi, G.; Garavelli, M. *Angew. Chem., Int. Ed.* **2010**, *49*, 1790−1793.

(5) (a) Freedman, K. A.; Becker, R. S. *J. Am. Chem. Soc.* **1986**, *108*, 1245−1251. (b) Koyama, Y.; Kubo, K.; Komori, M.; Yasuda, H.; Mukai, Y. *Photochem. Photobiol.* **1991**, *54*, 433−443.

(6) Kawanabe, A.; Kandori, H. *Sensors* **2009**, *9*, 9741−9804.

(7) (a) Govindjee, R.; Balashov, S. P.; Ebrey, T. G. *Biophys. J.* **1990**, *58*, 597−608. (b) Logunov, S. L.; El-Sayed, M. A. *Phys. Chem. B* **1997**, *101*, 6629−6633. (c) Kim, J. E.; Tauber, M. J.; Mathies, R. A. *Biochemistry* **2001**, *40*, 13774−13778. (d) Losi, A.; Wegener, A. A.; Engelhard, M.; Braslavsky, S. E. *Photochem. Photobiol.* **2001**, *74*, 495−503. (e) Rupenyan, A.; van Stokkum, I. H. M.; Arents, J. C.; van Grondelle, R.; Hellingwerf, K.; Groot, M. L. *Biophys. J.* **2008**, *94*, 4020−4030.

(8) Groma, G. I.; Hebling, J.; Kozma, I. Z.; Varo, G.; Hauer, J.; Kuhl, J.; Riedle, E. *Proc. Natl. Acad. Sci. U.S.A.* **2008**, *105*, 6888−6893.

(9) Kobayashi, T.; Kim, M.; Taiji, M.; Iwasa, T.; Nakagawa, M.; Tsuda, M. *J. Phys. Chem. B* **1998**, *102*, 272−280.

(10) Zgrablić, G.; Haacke, S.; Chergui, M. J. *Phys. Chem. B.* **2009**, *113*, 4384−4393.

(11) Kochendoerfer, G. G.; Mathies, R. A. *Isr. J. Chem.* **1995**, *35*, 211−226.

(12) Stuart, J. A.; Birge, R. R. Characterization of the Primary Photochemical Events in Bacteriorhodopsin and Rhodopsin. In *Biomembranes*; Lee, A. G., Ed.; JAI Press: London, 1996; pp 33−139.

(13) Neumann, K.; Verhoefen, M. K.; Weber, I.; Glaubitz, C.; Wachtveitl, J. *Biophys. J.* **2008**, *94*, 4796−4807.

(14) Lutz, I.; Sieg, A.; Wegener, A. A.; Engelhard, M.; Boche, I.; Otsuka, M.; Oesterhelt, D.; Wachtveitl, J.; Zinth, W. *Proc. Natl. Acad. Sci. U.S.A.* **2001**, *98*, 962−967.

(15) Kandori, H.; Tomioka, H; Sasabe, H. *J. Phys. Chem. A* **2002**, *106*, 2091−2095.

(16) (a) Hamm, P.; Zurek, M.; Roschinger, T.; Patzelt, H.; Oesterherlt, D.; Zinth, W. *Chem. Phys. Lett.* **1996**, *263*, 613−621. (b) Hamm, P.; Zurek, M.; Roschinger, T.; Patzelt, H.; Oesterherlt, D.; Zinth, W. *Chem. Phys. Lett.* **1997**, *268*, 180−186.

(17) Bismuth, O.; Friedman, N.; Sheves, M.; Ruhman, S. *Chem. Phys.* **2007**, *341*, 267−275.

(18) Amsden, J. J.; Kralj, J. M.; Chieffo, L. R.; Wang, X.; Erramilli, S.; Spudich, E. N.; Spudich, J. L.; Ziegler, L. D.; Rothschild, K. J. *J. Phys. Chem. B* **2007**, *111*, 11824−11831.

(19) Hou, B.; Friedman, N.; Ruhman, S.; Sheves, M.; Ottolenghi, M. *J. Phys. Chem. B* **2001**, *105*, 7042−7048.

(20) Logunov, S. L.; Song, L.; El-Sayed, M. *J. Phys. Chem.* **1996**, *100*, 18586−18591.

(21) Kandori, H.; Katsuta, Y.; Ito, M.; Sasabe, H. *J. Am. Chem. Soc.* **1995**, *117*, 2669−2670.

(22) Logunov, S. L.; El-Sayed, M. A. *Phys. Chem. B* **1997**, *101*, 6629−6633.

(23) Petrich, J. W.; Breton, J.; Martin, J. L.; Antonetti, A. *Chem. Phys. Lett.* **1987**, *137*, 369−375.

(24) Dobler, J.; Zinth, W.; Kaiser, W.; Oesterhelt, D. *Chem. Phys. Lett.* **1988**, *144*, 215−220.

(25) Mathies, R. A.; Cruz, B. C. H.; Pollard, W. T.; Shank, C. V. *Science* **1988**, *240*, 777−779.

(26) Kobayashi, T.; Kim, M.; Taiji, M.; Iwasa, T.; Nakagawa, M.; Tsuda, M. *J. Phys. Chem. B* **1998**, *102*, 272−280.

(27) Haran, G.; Wynne, K.; Xie, A.; He, Q.; Chance, M.; Hochstrasser, R. M. *Chem. Phys. Lett.* **1996**, *261*, 389−395.

(28) Haacke, S.; Vinzani, S.; Schenkl, S.; Chergui, M. *ChemPhysChem* **2001**, *2*, 310−315.

(29) Schmidt, B.; Sobotta, C.; Heinz, B.; Laimgruber, S.; Braun, M.; Gilch, P. *Biochim. Biophys. Acta* **2005**, *1706*, 165−173.

(30) (a) Hasson, K. C.; Gai, F.; Anfinrud, P. A. *Proc. Natl. Acad. Sci. U.S.A.* **1996**, *93*, 15124−15129. (b) Gai, F.; Hasson, K.; McDonald, J. C.; Anfinrud, P. A. *Science* **1998**, *279*, 1886−1891.

(31) Wand, A.; Friedman, N.; Sheves, M.; Ruhman, S. *J. Phys. Chem. B* **2012**, *116*, 10444−10452.

(32) Ruhman, S.; Hou, B.; Friedman, N.; Ottolenghi, M.; Sheves, M. *J. Am. Chem. Soc.* **2002**, *124*, 8854−8858.

(33) Briand, J.; Léonard, J.; Haacke, S. *J. Opt.* **2010**, *12*, 084004.

(34) Losy, A.; Wegener, A. A.; Engelhard, M.; Braslavsky, S. E. *Photochem. Photobiol.* **2001**, *74*, 495−503.

(35) Sovdat, T.; Bassolino, G.; Liebel, M.; Schnedermann, C.; Fletcher, S. P.; Kukura, P. *J. Am. Chem. Soc.* **2012**, *134*, 8318−8320.

(36) Briand, J.; Bram, O.; Rehault, J.; Léonard, J.; Cannizzo, A.; Chergui, M.; Zanirato, V.; Olivucci, M.; Helbing, J.; Haacke, S. *Phys. Chem. Chem. Phys.* **2010**, *12*, 3178−3187.

(37) Kobayashi, T.; Saito, T.; Ohtani, H. *Nature* **2001**, *414*, 531−534.
(38) Warshel, A.; Chu, Z. T. *J. Phys. Chem. B* **2001**, *105*, 9857−9871.
(39) Gonzalez-Luque, R.; Garavelli, M.; Bernardi, F.; Merchán, M.; Robb, M. A.; Olivucci, M. *Proc. Natl. Acad. Sci. U.S.A.* **2000**, *97*, 9379−9384.
(40) Humphrey, W.; Logunov, L. H.; Werner, H. J.; Schulten, K. *Biophys. J.* **1998**, *75*, 1689−1699.
(41) Ben-Nun, M.; Molnar, F.; Lu, H.; Phillips, J. C.; Martínez, T. J.; Schulten, K. *Faraday Discuss.* **1998**, *110*, 447−462.
(42) Hayashi, S.; Tajkhorshid, E.; Schulten, K. *Biophys. J.* **2003**, *85*, 1440−1449.
(43) Bismuth, O.; Komm, P.; Friedman, N.; Eliash, T.; Sheves, M.; Ruhman, S. *J. Phys. Chem. B* **2010**, *114*, 3046−3051.
(44) (a) Zgrablić, G.; Voïtchovsky, K.; Kindermann, M.; Haacke, S.; Chergui, M. *Biophys. J.* **2005**, *88*, 2779−2788. (b) Zgrablić, G.; Haacke, S.; Chergui, M. *Chem. Phys.* **2007**, *338*, 168−174.
(45) (a) Polívka, T.; Sundström, V. *Chem. Rev.* **2004**, *104*, 2021−2072. (b) Polívka, T.; Herek, J. L.; Zigmantas, D.; Aikerlund, H.-E.; Sundström, V. *Proc. Natl. Acad. Sci. U.S.A.* **1999**, *96*, 4914.
(46) Garavelli, M. *Theor. Chem. Acc.* **2006**, *116*, 87−105.
(47) Loevsky, B.; Wand, A.; Biismuth, O.; Friedman, N.; Sheves, M.; Ruhman, S. J. *Am. Chem. Soc.* **2011**, *133*, 1626−1629.
(48) The vibrational combination bands of water absorb significantly at $\lambda > 1600$ nm, preventing collection of reliable transient absorption spectra at this spectral region. Extension to longer wavelengths for the case of RPSB, which is dissolved in an ethanol solution, can be found in the communication by Loevsky et al. (ref 47).
(49) Jung, K.-H.; Trivedi, V. D.; Spudich, J. L. *Mol. Microbiol.* **2003**, *47*, 1513−1522.
(50) Wand, A.; Rozin, R.; Eliash, T.; Jung, K.-H.; Sheves, M.; Ruhman, S. *J. Am. Chem. Soc.* **2011**, *133*, 20922−20932.
(51) Oesterhelt, D.; Stoeckenius, W. In *Biomembranes Part A*; Sidney Fleischer, L. P., Ed.; Academic Press: New York, 1974; Vol. *31*, pp 667−678.
(52) Choi, A. R.; Kim, S. Y.; Yoon, S. R.; Bae, K.; Jung, K.-H. *Microbiol. Biotechnol.* **2007**, *17*, 138−145.
(53) Kovalenko, S. A.; Dobryakov, A. L.; Ruthmann, J.; Ernsting, N. P. *Phys. Rev. A* **1999**, *59*, 2369−2384.
(54) Polli, D.; Brida, D.; Mukamel, S.; Lanzani, G.; Cerullo, G. *Phys. Rev. A* **2010**, *82*, 053809.
(55) Nakamura, T.; Takeuchi, S.; Shibata, M.; Demura, M.; Kandori, H.; Tahara, T. *J. Phys. Chem. B* **2008**, *112*, 12795−12800.
(56) Mukamel, S. *Principles of Nonlinear Optical Spectroscopy*; Oxford University Press: New York, 1995.
(57) Wand, A.; Kallush, S.; Shoshanim, O.; Bismuth, O.; Kosloff, R.; Ruhman, S. *Phys. Chem. Chem. Phys.* **2010**, *12*, 2149−2163.
(58) Some phase shift of the oscillations is apparent between $\lambda_{pr} \approx$ 950−1100 nm. This shift amounts to only a fraction of the relevant low-frequency vibrational modes, and therefore these were averaged for improving the S/N of the following analysis.
(59) Hou, B.; Friedman, N.; Ottolenghi, M.; Sheves, M.; Ruhman, S. *Chem. Phys. Lett.* **2003**, *381*, 549−555.
(60) (a) Kraack, J. P.; Buckup, T.; Motzkus, M. *Phys. Chem. Chem. Phys.* **2011**, *13*, 21402−21410. (b) Kraack, J. P.; Buckup, T.; Hampp, N.; Motzkus, M. *ChemPhysChem* **2011**, *12*, 1851−1859.
(61) Polli, D.; Altoe, P.; Weingart, O.; Spillane, K. M.; Manzoni, C.; Brida, D.; Tomasello, G.; Orlandi, G.; Kukura, P.; Mathies, R. A.; Garavelli, M.; Cerullo, G. *Nature* **2010**, *467*, 440−443.
(62) Li, X.; Chung, L. W.; Morokuma, K. *J. Chem. Theory Cumput.* **2011**, *7*, 2694−2698.
(63) Smith, S. O.; Braiman, M. S.; Myers, A. B.; Pardoen, J. A.; Courtin, J. M. L.; Winkel, C.; Lugtenburg, J.; Mathies, R. A. *J. Am. Chem. Soc.* **1987**, *109*, 3108−3125.
(64) Pollard, W. T.; Dexheimer, S. L.; Wang, Q.; Peteanu, L. A.; Shank, C. V.; Mathies, R. A. *J. Phys. Chem.* **1992**, *96*, 6147−6158.
(65) Song, L.; El-Sayed, M. A. *J. Am. Chem. Soc.* **1998**, *120*, 8889−8890.
(66) Kobayashi, T.; Saito, T.; Ohtani, H. *Nature* **2001**, *414*, 531−534.
(67) (a) McCamant, D. W.; Kukura, P.; Mathies, R. A. *J. Phys. Chem. B* **2005**, *109*, 10449−10457. (b) Shim, S.; Dasgupta, J.; Mathies, R. A. *J. Am. Chem. Soc.* **2009**, *131*, 7592−7597.
(68) Schapiro, I.; Ryazantsev, M. N.; Frutos, L. M.; Ferré, N.; Lindh, N.; Olivucci, M. *J. Am. Chem. Soc.* **2011**, *133*, 3354−3364.
(69) Lin, S. W.; Groesbeek, M.; van der Hoef, I.; Verdegem, P.; Lugtenburg, J.; Richard, A.; Mathies, R. A. *J. Phys. Chem. B* **1998**, *102*, 2787−2806.
(70) Cembran, A.; Bernardi, F.; Olivucci, M.; Garavelli, M. *J. Am. Chem. Soc.* **2003**, *125*, 12509−12519.
(71) Hou, B.; Friedman, N.; Ottolenghi, M.; Sheves, M.; Ruhman, S. *Chem. Phys. Lett.* **2003**, *381*, 549−555.
(72) Kahan, A.; Nahmias, O.; Friedman, N.; Sheves, M.; Ruhman, S. *J. Am. Chem. Soc.* **2007**, *129*, 537−546.
(73) Ye, T.; Gershgoren, E.; Friedman, N.; Ottolenghi, M.; Sheves, M.; Ruhman, S. *Chem. Phys. Lett.* **1999**, *314*, 429−434.
(74) Herz, J.; Verhoefen, M.-K.; Weber, I.; Bamann, C.; Glaubitz, C.; Wachtveitl. *J. Biochem.* **2012**, *51*, 5589−5600.
(75) (a) Myers, A. B.; Harris, R. A.; Mathies, R. A. *J. Chem. Phys.* **1983**, *79*, 603−613. (b) Loppnow, G. R.; Mathies, R. A.; Middendorf, T. R.; Gottfried, D. S.; Boxer, S. G. *J. Phys. Chem.* **1992**, *96*, 737−745. (c) Smith, S. O.; Myers, A. B.; Mathies, R. A.; Pardoen, J. A.; Winkel, C.; van den Berg, E. M. M.; Lugtenburg, J. *Biophys. J.* **1985**, *47*, 653−664.
(76) Kraack, J. P.; Buckup, T.; Motzkus, M. *Phys. Chem. Chem. Phys.* **2012**, *14*, 13979−13988.
(77) (a) Prokhorenko, V. I.; Nagy, A. M.; Waschuk, S. A.; Brown, L. S.; Birge, R. R.; Miller, R. J. D. *Science* **2006**, *313*, 1257−1261. (b) Prokhorenko, V. I.; Nagy, A. M.; Brown, L. S.; Miller, R. J. D. *Chem. Phys.* **2007**, *341*, 296−309.
(78) Kumar, A. T. N.; Rosca, F.; Widom, A.; Champion, P. A. *J. Chem. Phys.* **2001**, *114*, 701−724.
(79) Gershgoren, E.; Vala, J.; Kosloff, R.; Ruhman, S. *J. Phys. Chem. A* **2001**, *105*, 5081−5095.